

LETTERS TO NATURE

Measurement of atmospheric wavefront distortion using scattered light from a laser guide-star

R. Q. Fugate*, D. L. Fried†, G. A. Ameer†,
 B. R. Boeke*‡, S. L. Browne†, P. H. Roberts†,
 R. E. Ruane*‡, G. A. Tyler† & L. M. Wopat*

* Starfire Optical Range, Phillips Laboratory/LTE, Kirtland AFB,
 New Mexico 87117-6008, USA

† Optical Sciences Company, PO Box 1329, Placentia,
 California 92670, USA

‡ Present address: Rockwell Power Systems, Albuquerque,
 New Mexico 87117, USA

THE possibility of using an artificial 'guide-star' to measure optical wavefront distortion caused by atmospheric turbulence has been discussed for some time¹⁻⁴, but few experimental data are available⁵. Here we report experimental results demonstrating that atmospheric wavefront distortion can be measured by taking fast 'snapshots' of a guide-star formed by light scattered from a laser beam focused in the upper atmosphere. These results agree with a theoretical prediction⁶ that the mean-square wavefront error created by using an artificial guide-star at a finite distance rather than a real (infinitely distant) star is proportional to the five-thirds power of the telescope aperture. Using this understanding of the physics, we have demonstrated continuous, real-time atmospheric compensation of a 1.5-m telescope using a high-pulse-rate laser, pulse-synchronized wavefront sensor and deformable mirror, and have been able to resolve the 1.3-arcsecond binary star 53 ξ Ursa Majoris in an exposure time of only one second.

The US Department of Defense has been developing laser guide-star adaptive optics since October 1981, but has allowed public release of information only since May 1991. The programme started following a suggestion made by Julius Feinleib of Adaptive Optics Associates for creating artificial stars from the Rayleigh scattering of a laser beam focused in the upper atmosphere. Because rays from the laser guide-star beacon may

travel along a different-path from those of the star under observation, the effects of atmospheric turbulence may be quite different in each case, resulting in focus anisoplanatism. Fried assessed the usefulness of such a finite-range guide-star, and showed that useful performance could be achieved even with the wavefront-distortion error caused by focus anisoplanatism. In 1982, laser excitation of mesospheric sodium was suggested⁹ as a means of generating artificial guide-stars at a significantly higher altitude to reduce the focus anisoplanatic error. The Defense Advanced Research Projects Agency (DARPA) sponsored two experiments—one to test the Rayleigh scattering idea and the other to test the resonant mesospheric sodium concept. Here we report the results of the Rayleigh guide-star experiment conducted at the Starfire Optical Range (SOR) in New Mexico during 1983. The sodium experiment was conducted at White Sands Missile Range, New Mexico, during 1984¹⁰. In 1985, independently of the work of the Department of Defense, the idea of using the Rayleigh and sodium laser guide-stars concepts was suggested¹. Thompson and Gardner⁵ generated a mesospheric sodium guide-star and verified radiometric predictions. In mid-1988, the Massachusetts Institute of Technology Lincoln Laboratory showed atmospheric compensation on a 0.6-m aperture using a Rayleigh laser guide-star operating at a few pulses per second and a special 'go-to' control system for their adaptive optics system. In February 1989, our group at Phillips Laboratory demonstrated high-bandwidth, closed-loop atmospheric compensation on the SOR 1.5-m telescope using a high-repetition-rate Rayleigh laser-guide-star. We analysed stellar images formed at an average wavelength of $0.88 \pm 0.05 \mu\text{m}$ while operating the adaptive optics at a closed-loop bandwidth of 30–65 Hz using a laser guide-star at a range of 10 km. We achieved Strehl ratios (ratio of actual peak intensity to diffraction limited peak intensity) of >0.2 , full-width-half-maximum resolution of 0.18 arcsec, and image intensity improvements of nearly an order of magnitude in the presence of visible wavelength atmospheric seeing conditions of 2 arcsec (R.Q.F. *et al.* manuscript in preparation). Figure 1 shows the improvement in a binary star image achieved with the laser guide-star adaptive optics operating on the 1.5-m telescope.

The primary objective of our first laser guide-star experiment performed in 1983 was to determine whether a laser beam focused in the atmosphere really could be used as a beacon to

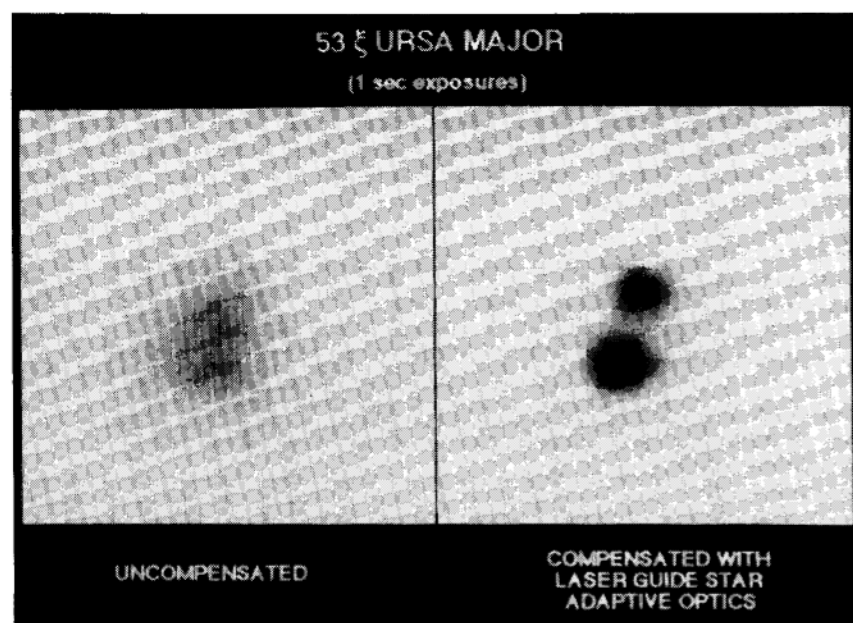
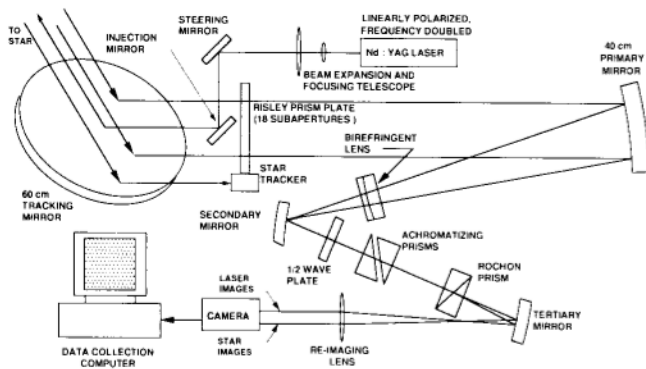


FIG. 1 Charge-coupled-device camera images of the binary star 53 ξ Ursa Majoris ($m_1=4.2$ and 4.5, separation ~ 1.3 arcsec) made through the SOR 1.5-m telescope. Each image is 6.24 arcsec square exposed for one second at an average wavelength of $0.88 \mu\text{m}$ and spectral bandwidth of $0.1 \mu\text{m}$. The laser guide-star adaptive optics was operated at 65-Hz closed-loop bandwidth. The peak intensity in the compensated image is 8.6 times the peak intensity in the uncompensated image. The Strehl ratio of the compensated image is ~ 0.1 and the full-width-half-maximum size of the bright star image is 0.48 arcsec. Full-width-half-maximum image sizes of <0.2 arcsec were achieved for exposures of ~ 20 ms. The degradation at long exposures is due largely to imperfect overall tilt compensation provided by a separate tracker and steering mirror.



measure atmospheric-turbulence-induced wavefront distortion, and to assess the quality of the measurement values it produced. The reference (or 'truth') results for this experiment were provided by simultaneous wavefront-distortion measurements using a star as the beacon. Wavefronts determined using the laser beacon were compared with simultaneous wavefront-distortion measurements made using on-axis starlight, the r.m.s. discrepancy between the two wavefronts being compared with theory. The optics were arranged so as to direct the laser beam within a few microradians of the star, thereby, ensuring that light from both the star and the laser guide-star beacons propagate through nearly identical turbulence.

Figure 2 shows the essential features of the experimental set-up. The tracking mirror was positioned by a two-axis gimbal-mounted under the control of a low-bandwidth star tracker which kept the optical axis of the 40-cm phase-measurement telescope within one microradian of the star's average position. We used the star Polaris for these experiments because the two-axis gimbal was limited to $\pm 1^\circ$ of total motion in each axis. The 300 mJ per pulse, Q-switched laser beam which we used was expanded to 10-cm diameter, in nearly collimated form, and directed out of the centre of the 40-cm wavefront-sensing aperture, and aligned to be parallel to its optical axis. The beam was focused at a range of 5 km for most tests and the sensor was range-gated to accept backscattered light from 4.5 to 5.5 km.

The wavefront sensor consisted of an 18 subaperture Hartmann-type arrangement, each subaperture defined by an 8-cm

FIG. 2 Schematic diagram of the experimental set-up used for Rayleigh laser guide-star measurements of atmospheric-turbulence-induced wavefront distortion. With the exception of the 60-cm tracking mirror, all components were mounted on a large optics table. The 40-cm-diameter wavefront-distortion-sensing telescope consisted of an off-axis paraboloidal primary mirror and a convex secondary mirror. Hartmann sensor subapertures for measurement of wavefront distortion were defined by 18 Risley prisms mounted in a large plate in front of the 40-cm primary mirror. The subapertures were arranged on two concentric circles with 12 on the outer ring and six on the inner ring. The telescope optics focused all the light on a split photocathode intensifier coupled to a charge-injection-device sensor array. Because of the different settings of each of the Risley prisms, 18 distinct images of a point source were formed. The set of 18 associated centroids defined the wavefront tilt at each of the subapertures. The birefringent lens compensated for the difference in focus between the laser and star beacons.

diameter Risley prism. The subaperture geometry consisted of two concentric circles with 12 subapertures on the outer circle and six on the inner circle. Each subaperture produced its own distinct image of a beacon, the location of each of the images being determined by the setting of the corresponding Risley prism. The prisms were rotated in their mounts to provide adequate space between the 18 subaperture images formed at the focal plane of the 40-cm diameter telescope. Two distinct sets of 18 such images were formed, one set being images of the laser guide-star and the other being images of the star.

To measure wavefront distortion simultaneously with the star and laser beacons, light from the two sources, after passing through the subapertures, was spatially separated by polarization, using the Rochon prism. This light, now sufficiently divided so as to be able to form two distinct sets of 18 spots, was imaged onto separate halves of a specially made, independently gated, split photocathode intensifier coupled to a charge-injection-device sensor array. All the light from the laser return was directed to one photocathode (where 18 suitably separated, laser spot images were formed) as the Rayleigh backscatter process does not depolarize the linearly polarized outgoing laser beam. The starlight was equally divided by the Rochon prism between the two halves of the photocathode as this light is randomly polarized—but the starlight going to the laser half of the photocathode was in effect neglected because of the shortness of the time for which that part of the photocathode was on. The laser-range gate was on for only a few microseconds,

FIG. 3 Representative sample of measured wavefront distortions and distortion difference. The lower-left plot shows the wavefront distortion measured using the starlight whereas the lower-right plot shows the wavefront distortion measured using the laser light—the Rayleigh laser guide-star. These distortions have mean square values of 4.434 rad^2 and 4.236 rad^2 respectively. The centre plot shows the difference between these two wavefronts. Its mean-square value of 0.363 rad^2 is a measure of the magnitude of the focus anisoplanatism—in this case for a 40 cm diameter aperture, viewing at a 35° elevation angle, using a guide-star at 5 km range, and with wavefronts corresponding to a wavelength of $0.53 \mu\text{m}$.

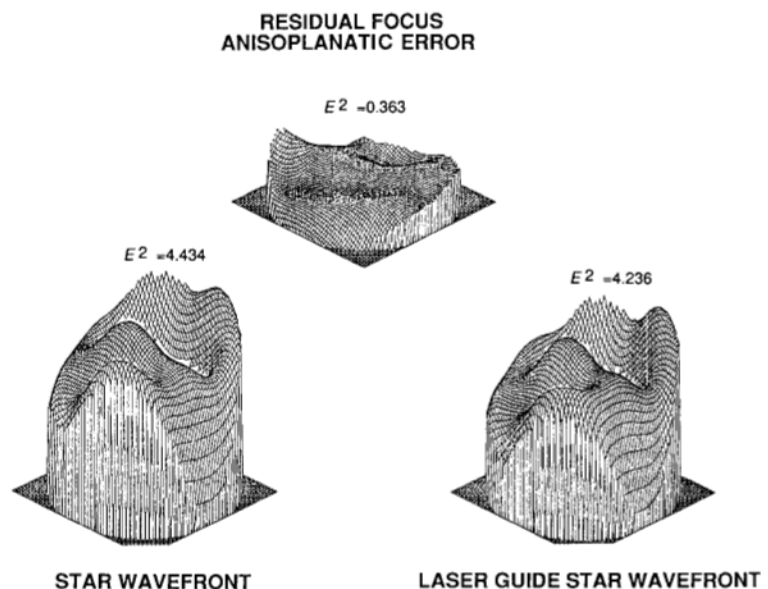
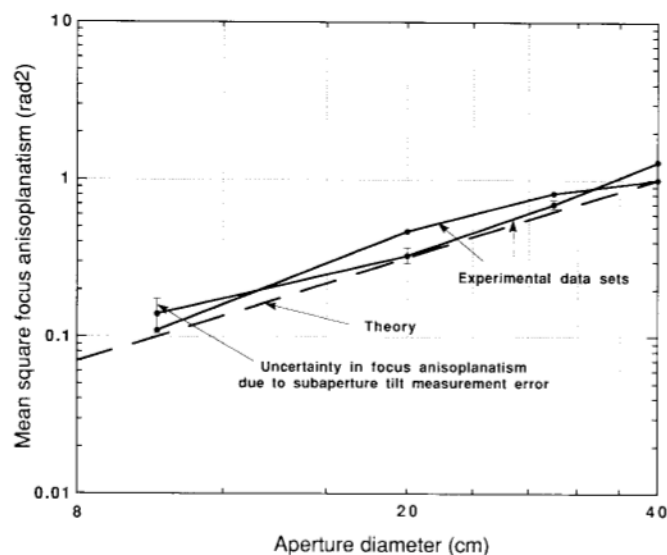


FIG. 4 Mean square focus anisoplanatism error. The term focus anisoplanatism refers to the fact that wavefront distortion measured with a laser guide-star will be somewhat different from what is needed to correct the turbulence induced wavefront distortion of light from a co-aligned star or other source more distant than the laser guide-star. When a laser guide-star is used to control an astronomical adaptive optics system, the focus anisoplanatism will result in a wavefront correction error. We show here the measured focus anisoplanatism for viewing a laser guide-star at 35° elevation and 5 km range, the error being expressed in radians² for a wavelength of 0.53 μm . The points shown represent two sets of data each formed by averaging over 35 wavefront distortion measurements. The broken straight line represents a theoretical prediction [cf. equation (1)] for which $d_0 = 0.39$ m. The measurement data not only shows the predicted five-thirds power dependence on aperture diameter, but also lies surprisingly close to the $d_0 = 0.39$ m theoretical curve. The uncertainty in our measurement of focus anisoplanatism is indicated by the error bars associated with one of the data sets. These errors were computed using a theoretical treatment of induced mean-square error associated with the difference of two reconstructed wavefronts [15, 16]. This theory utilizes the rms subaperture tilt measurement error—experimentally determined for this experiment to be 650 nanoradians by comparison of identical wavefront exposures (i.e. star-star and laser-laser) on each half of the split photocathode sensor. The subaperture tilt error was dominated by sensor noise and the fact that the size of the laser-guide-star images were somewhat larger than the diffraction limit.



whereas the starlight gate had to be on for a few milliseconds in order to collect enough light. The starlight gate 'on' period was centred in time on the laser range gate (but was off during the laser firing period). Using this timing and polarization arrangement, only starlight images were formed on one side of the split photocathode, and only laser light images on the other. The birefringent lens compensated the focus for the difference in range to the laser and to the star beacons. A desktop computer and custom-made timing electronics controlled the laser firing, the individual photocathode gating, and the digital data collection by a frame grabber attached to the charge-injection-device sensor.

We processed many frames of raw image data to determine, for each, the centroid position of each spot and thus the tilts (wavefront gradients) for each subaperture. The gradient data were used to reconstruct the wavefront distortion over the 40-cm aperture, once for the laser beacon data and once for the star data. Figure 3 is a representative example of the wavefront distortion as determined for the star (truth) and for the laser beacon; also shown is the difference between these two, corresponding to what would be the residual error in an adaptive-optics-corrected star wavefront if the laser-beacon data had been used to control the deformable mirror used in the adaptive optics set-up. These results demonstrate qualitatively that laser guide-star beacons are effective in measuring atmospheric-turbulence-induced wavefront distortion.

Theoretical analysis carried out before this experiment predicted that the mean square difference between the tilt-removed laser-beacon wavefront distortion and the star-beacon wavefront distortion should increase with aperture diameter to the five-thirds power⁶. According to theory, a constant of proportionality, d_0 , was defined in such a way that

$$\langle E^2 \rangle = (D/d_0)^{5/3} \quad (1)$$

where D is the aperture diameter and $\langle E^2 \rangle$ is the aperture-averaged square phase difference between the star wavefront and the laser-beacon wavefront, ensemble averaged over turbulence realizations. The parameter d_0 depends on the wavelength of interest, the height of the laser beacon above the ground, and the height dependence of the index of refraction structure function, C_N^2 . Physically, one can think of d_0 as the size of a real aperture for which the wavefront

error incurred by using the laser guide-star would be one radian (r.m.s.).

Equation (1) represents the mean square error incurred by using the laser guide-star beacon when a real guide-star beacon is not available for use by an adaptive optics system. The error results from the fact that the two sources are at different ranges so rays from the two sources follow different paths through the atmosphere to each point in the aperture. Consequently, at the edge of the aperture, rays from the laser beacon sample the atmospheric turbulence along a (potentially significantly) different path than do rays from the star. Figure 4 shows $\langle E^2 \rangle$ derived from the experimental measurements, as a function of aperture diameter¹³. The experimental data are in excellent agreement with the theory predicting a $D^{5/3}$ dependence.

The value of d_0 is easily calculated from the data in Fig. 4 and equation (1) as being 0.39 m. The theoretical estimate of d_0 for our wavelength, zenith angle and backscatter altitude, using a nighttime turbulence profile model is 0.39 m¹⁴. Experiments performed in more benign atmospheric conditions and with a range gate at 15 km, produced mean-square-wavefront errors as low as 0.18 rad² and a d_0 of 1.1 m, which is good enough to allow wavefront correction to 1/15 of a wave over our 40-cm aperture. □

Received 23 May; accepted 6 August 1991.

1. Foy, R. & Labeyrie, A. *Astr. Astrophys.* **152**, L29-L31 (1985).
2. Séchaud, M. et al. in *Very Large Telescopes and their Instrumentation*, Proceedings Vol II (ed Ulrich, M. H.) 705-714 (European Southern Observatory, Garching, 1988).
3. Beckers, J. M. in *Very Large Telescopes and their Instrumentation*, Proceedings Vol II (ed Ulrich, M. H.) 693-703 (European Southern Observatory, Garching, 1988).
4. Gardner, C. S., Welsh, B. M. & Thompson, L. A. *Proc. IEEE* **78**, 1721-1743 (1990).
5. Thompson, L. A. & Gardner, C. S. *Nature* **328**, 229-231 (1987).
6. Belsher, J. F. & Fried, D. L. *Rep. No. TR-576* (Optical Sciences Company Placentia, 1984).
7. Fugate, R. Q. et al. *Bull. Am. Astr. Soc.* **23**(2), 898 (1991).
8. Fried, D. L. & Roberts, P. H. *Rep. No. TR-460* (Optical Sciences Company Placentia, 1982).
9. Happer, W. & MacDonald, G. *JASON Rep. No. JSR-82-106* (MITRE Corp, McLean 1983).
10. Humphreys, R. A. et al. *Optics Lett.* (submitted).
11. Primmerman, C. A., *Bull. Amer. Astr. Soc.* **23**(2), 898 (1991).
12. Primmerman, C. A. et al. *Nature* **353**, 141-143 (1991).
13. Fugate, R. Q. et al. *High Energy Laser Review Group/Propagation Sub-Panel Adaptive Optics Workshop* (Albuquerque, 1984).
14. Tyler, G. A. *Rep. No. TR-582* (Optical Sciences Company, Placentia, 1984).
15. Tyler, G. A. 1983 *Rep. No. TR-545* (Optical Sciences Company, Placentia, 1983).
16. Tyler, G. A. & Fried, D. L. *Rep. No. TR-514* (Optical Sciences Company, Placentia 1983).

ACKNOWLEDGEMENTS. We thank Rhetttig P. Benedict Jr and other DARPA officials for sponsoring parts of this work and Donald Hanson of the Air Force Rome Air Development Center for technical discussions and loan of critical test equipment.